Analysis and Design of Lumped- and Lumped-Distributed-Element Directional Couplers for MIC and MMIC Applications

Ryszard W. Vogel, *Senior Member, IEEE*

Abstract—**An analysis of lumped- and lumped-distributed-element directional couplers is described. The assumed generality of the ring type four-port enables different types of directionality to be developed. The equations enabling an idealized design of co-, contra- and trans-directional couplers for arbitrary power division and transformation ratio are derived. A design procedure for three-branch, lumped-element directional couplers, which enables an impedance transformation between the input and output, ports is also included. Computer simulations of the performance of various couplers with lumped elements represented by realistic models are included in the paper.**

I. Introduction

CONVENTIONAL directional couplers are realized with the use of transmission lines of different types. In MIC and MMIC constructions microstrip lines are the most popular. At frequencies below 20 GHz distributed components occupy large areas and create dimensional problems in MMIC's. Lumped elements are very attractive in applications where size reduction is important. It is known [1] that, at a single frequency, the symmetrical π − or T − LC section is equivalent to the transmission line section with the appropriate characteristic impedance and length. Consequently, the lines which compose a coupler can be partially or completely replaced by lumped sections [1]–[4]. In certain applications directional couplers with unequal terminal impedances have been constructed [5], [6]; lumped-element equivalents are attractive here because large transformation ratios are achievable.

This paper is organized as follows. In Section II, equations enabling the analysis of a symmetrical four-port network with lumped-distributed elements are derived. These equations and the conditions given in the Appendix are used in Section III to derive idealized design rules for co-directional (COD), contradirectional (CTD) and transdirectional (TRD) couplers. Three particular structures, lumped-element (LE), lumped-distributed element (LDE) and distributed-lumped element (DLE) networks, are considered. The analysis indicates that various types of networks fulfill the conditions required for an ideal coupler. Therefore, greater design flexibility in the choice of the coupler structure and performance is possible. These possibilities have not previously been indicated in the literature. The equations presented in the paper are useful for preliminary design of the circuits while final design can be refined with the help of commercially available simulators. Section IV provides design equations for three-branch LE coupler-transformers which allow realization of much wider bandwidths and larger transformation ratios than achievable with two-branch LE couplers. Finally, in Section V, simulations concerning the properties of selected couplers using available models of inductors and capacitors illustrate the analysis. One of the examples—LDE CTD coupler, has much better performance than the classical $(3/2)\lambda$ ring coupler, demonstrating the design rules given in the paper allow one to develop new alternatives to commonly know devices.

Manuscript received September 10, 1990; revised July 22, 1991.

The author was with the Swedish Institute of Microelectronics, Stockholm, Sweden. He is now with NobelTech, Microwave Department, S-175 88, Järfälla, Sweden.

IEEE Log Number 9104765.

II. Wave-Amplitude Transmission Matrix Representation

The equivalent circuit of a symmetrical four-port network with lumped-distributed elements of the ring-type structure is shown in Fig. 1. Z_i and θ_i designate the characteristic impedances and electrical lengths of the transmission lines, respectively; X_{12}, B_i, B_{pi} are the lumped reactance and susceptances and Z_{01}, Z_{02} are the terminating impedances. This network can be analyzed by the even and odd modes method described by Reed and Wheeler [7]. The equivalent circuits of the two-ports for even and odd excitation are shown in Fig. 2. To determine the reflection and transmission coefficients of the circuits the transmission wave matrix description [8] is used. The transmission wave matrix of the two-port is given by

$$[T_{e,o}] = [T_{1e,o}][T_3][T_{12}][T_3][T_{2e,o}], \tag{1}$$

where the constituent T − matrices are given by

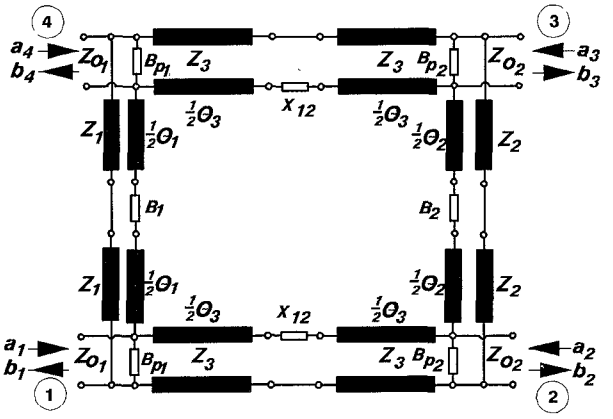

Fig. 1. Equivalent circuit of a general ring-type four-port with lumped-distributed elements.

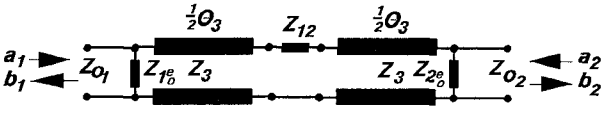

Fig. 2. Equivalent scheme of even- and odd-mode two-ports which represent the ring-type four-port with lumped-distributed elements.

$$\Im T_{11e,o} = \frac{1}{4}[(b_{1e,o} + b_{2e,o})A + B(1 - b_{1e,o}b_{2e,o}) + C],$$

$$\Re T_{12e,o} = \frac{1}{4\sqrt{n}}[(n-1)A + B(b_{1e,o} - nb_{2e,o})],$$

$$\Im T_{12e,o} = \frac{1}{4}[(b_{1e,o} + b_{2e,o})A - B(1 + b_{1e,o}b_{2e,o}) + C], \quad (3)$$

where

$$A = 2\cos\theta_3 - \frac{x_{12}}{z_3}\sin\theta_3;$$

$$B = 2z_3\sin\theta_3 + x_{12}(1 + \cos\theta_3),$$

$$C = \frac{1}{z_3^2}[2z_3\sin\theta_3 - x_{12}(1 - \cos\theta_3)]; \quad n = \frac{Z_{02}}{Z_{01}}.$$

Substituting these T_{ij} in the corresponding equations in the Appendix leads to conditions which have to be fulfilled to obtain the required type of directionality. Implementing these conditions into (A1) and (A2) one can calculate the frequency characteristics of the coupler. The duals to (1)–(3) may be obtained by interchanging $[T_e]$ and $[T_o]$, and replacing z_i, Z_{0i} with y_i, Y_{0i}.

$$[T_{1e,o}] = \frac{1}{2}\sqrt{\frac{Z_3}{Z_{01}}}\begin{bmatrix} 1 + Z_{01}(Y_3 + Y_{1e,o}) & 1 - Z_{01}(Y_3 - Y_{1e,o}) \\ 1 - Z_{01}(Y_3 + Y_{1e,o}) & 1 + Z_{01}(Y_3 - Y_{1e,o}) \end{bmatrix},$$

$$[T_3] = \begin{bmatrix} \exp\left(j\frac{\theta_3}{2}\right) & 0 \\ 0 & \exp\left(-j\frac{\theta_3}{2}\right) \end{bmatrix},$$

$$[T_{12}] = \frac{1}{2}\begin{bmatrix} 2 + Y_3Z_{12} & -Y_3Z_{12} \\ Y_3Z_{12} & 2 - Y_3Z_{12} \end{bmatrix},$$

$$[T_{2e,o}] = \frac{1}{2}\sqrt{\frac{Z_{02}}{Z_3}}\begin{bmatrix} 1 + Z_3(Y_{02} + Y_{2e,o}) & 1 - Z_3(Y_{02} - Y_{2e,o}) \\ 1 - Z_3(Y_{02} + Y_{2e,o}) & 1 + Z_3(Y_{02} - Y_{2e,o}) \end{bmatrix},$$

in which the $Y_{ie,o}$ ($i = 1, 2$) are the admittances introduced by the parallel coupling elements for the even ("e") and odd ("o") excitation, respectively.

Introducing the normalization

$$z_{ie,o} = (y_{ie,o})^{-1} = \frac{Z_{ie,o}}{\sqrt{Z_{01}Z_{02}}},$$

$$z_{12} = \frac{Z_{12}}{\sqrt{Z_{01}Z_{02}}}, \quad z_i = \frac{Z_i}{\sqrt{Z_{01}Z_{02}}}. \quad (2)$$

and assuming lossless elements i.e., $y_{ie,o} = jb_{ie,o}$, $z_{12} = jx_{12}$, one can express the elements of the transmission matrix $[T_{e,o}]$ as

$$T_{ije,o} = \Re T_{ije,o} + j\Im T_{ije,o},$$

$$\Re T_{11e,o} = \frac{1}{4\sqrt{n}}[(n+1)A - B(b_{1e,o} + nb_{2e,o})],$$

III. Directional Properties of Four-Port Networks with Lumped and Distributed Elements

Three types of networks resulting from Fig. 1 can be considered separately. The first consists of lumped elements (LE) only. The expressions (3) hold with the following substitutions:

$$\theta_3 = 0; \quad \theta_i = 0; \quad b_{ie} = b_{pi};$$

$$b_{io} = b_{pi} + 2b_i; \quad i = 1, 2. \quad (4a)$$

For the second, with lumped-distributed elements (LDE), the substitutions are

$$x_{12} = 0; \quad \theta_i = 0; \quad b_{ie} = b_{pi};$$

$$b_{io} = b_{pi} + 2b_i; \qquad i = 1, 2, \tag{4b}$$

and the third, with distributed-lumped elements (DLE), is described by

$$\theta_3 = 0; \quad b_{ie} = b_{pi} + y_i t_i;$$

$$b_{io} = b_{pi} - y_i t_i^{-1} \quad \text{where} \quad t_i = \tan\frac{\theta_i}{2}. \tag{4c}$$

A. Codirectional Couplers ($S_{ii} = S_{14} = 0$)

1) LE Network (4a): Solution of (A8) leads to the relations

$$b_{1c} = nb_{2c}; \quad x_{12c} = \frac{1}{b_{1c} + b_{p1c}} = \frac{1}{b_{2c} + b_{p2c}}; \quad x_{12c}^2 = \frac{1}{1 + nb_{p2c}^2} \tag{5}$$

which assure the codirectionality. The scattering coefficients representing the transmission and coupling are given by

$$S_{12c} = -jx_{12c}; \quad S_{13c} = \sqrt{n}b_{2c}x_{12c} = \pm\sqrt{1 - x_{12c}^2}. \tag{6}$$

The subscript c indicates that the equations apply at the center frequency ($f = f_c$) only. Consequently, the frequency characteristics of the coupler are selective and their shapes depend on the kinds of reactive elements selected. Fig. 3 illustrates the possible coupler options which fulfill the conditions (5). It should be remarked that the networks shown in Fig. 3(e) and (f) can be realized only when $n \neq 1$. The circuits presented in Fig. 3(b), (d), and (f) are obtained from the circuits shown in Fig. 3(a), (c), and (e) by interchanging inductors and capacitors, thereby inverting the frequency characteristics ($f/f_c \rightarrow f_c/f$).

2) LDE Network (4b): The following expressions assure codirectionality of the LDE network:

$$z_3 \tan\theta_{3c} = \frac{1}{(b_{1c} + b_{p1c})} = \frac{1}{(b_{2c} + b_{p2c})};$$

$$b_{1c} = nb_{2c}; \quad z_3^2 \sin^2\theta_{3c} = \frac{1}{1 + nb_{2c}^2}. \tag{7}$$

The scattering coefficient defining the coupling is equal to

$$S_{13c} = \sqrt{n}b_{2c}z_3 \sin\theta_{3c} = \sqrt{1 - z_3^2 \sin^2\theta_{3c}}. \tag{8}$$

According to (7), different coupler configurations are possible, and, their frequency behavior can be interpreted similar to the previous case.

3) DLE Network (4c): This network becomes a COD coupler if

$$nz_1 \sin\theta_{1c} = z_2 \sin\theta_{2c}; \quad x_{12c}^2 = \frac{nz_1^2 \sin^2\theta_{1c}}{1 + nz_1^2 \sin^2\theta_{1c}}, \tag{9a}$$

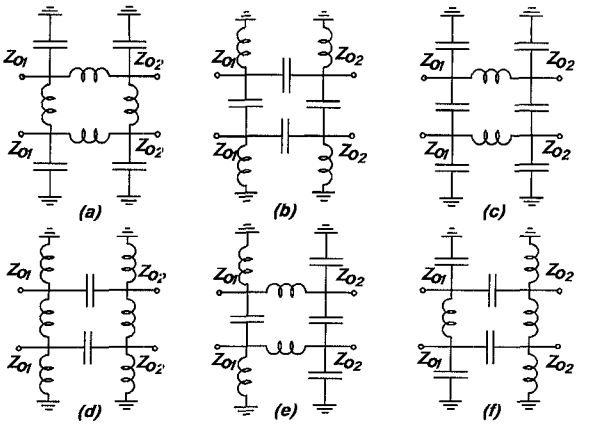

Fig. 3. Equivalent circuits of LE COD couplers.

$$\frac{1}{x_{12c}} = b_{p1c} - y_1 \cot\theta_{1c} = b_{p2c} - y_2 \cot\theta_{2c}. \tag{9b}$$

The coupling can be calculated according to

$$S_{13c} = -\frac{x_{12c}}{\sqrt{n}z_1 \sin\theta_{1c}} = \mp\sqrt{1 - x_{12c}^2}. \tag{10}$$

As may be seen from (6), (8), and (10), the series reactances x_{12c} or the characteristic impedance z_3 are directly related to the desired coupling. Then, the rest of the parameters can be determined. The last network considered gives an additional degree of freedom i.e., the product of $z_i \sin\theta_i$ is determined, and one of these parameters may be chosen arbitrarily, taking into account the physical limitations only.

B. Contradirectional Couplers ($S_{11} = S_{13} = 0$)

Considering the contradirectional case one can find that this feature is achievable for LE, LDE, and DLE circuits. It can be easily checked that the realization of the quadrature coupler is impossible and only a magic-T case will be considered.

1) LE Network: The equations which result from the conditions (A11) and (A14) are

$$b_{1c} = -nb_{2c}; \quad x_{12c} = \frac{1}{b_{1c} + b_{p1c}} = \frac{1}{b_{2c} + b_{p2c}};$$

$$x_{12c}^2 = \frac{1}{1 - b_{2c}^2} \tag{11}$$

and make the output signals to be in or out of phase. The coupling is calculated from

$$S_{14c} = j\sqrt{n}b_{2c}. \tag{12}$$

Fig. 4 shows possible configurations of the circuits which can fulfill the above equations. It is seen that the networks shown in Fig. 4(b) and (d) are derived from the networks presented in Fig. 4(a) and (c), as a result of the frequency inversion. It can also be noticed that some simplification of these schemes is possible e.g., for $C = 3$ dB and $n =$

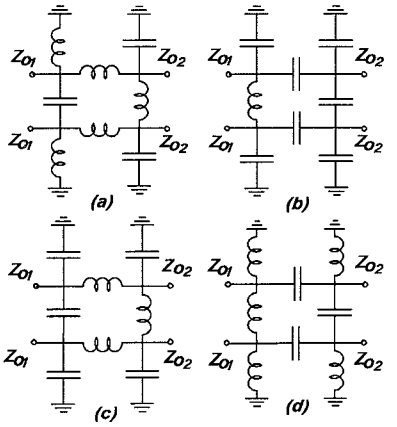

Fig. 4. Equivalent circuits of LE CTD couplers.

1, one pair of the shunting susceptances (b_{p1} or b_{p2}) is eliminated.

2) LDE Network: This type of network can be contradirectional with 0° or 180° phase relations if its parameters fulfill the following equations:

$$b_{1c} = -nb_{2c};\quad b_{1c} + b_{p1c} = n(b_{2c} + b_{p2c});$$

$$\theta_{3c} = (2k+1)\frac{\pi}{2};\quad z_3^2 = \frac{1}{1 + b_{p1c}b_{p2c}} \tag{13}$$

where $k = 0, 1, 2, \cdots$. The scattering coefficients can be determined from

$$S_{14c} = \frac{b_{1c}}{(b_{1c} + b_{p1c}) - j\sqrt{n}} = -\frac{z_3 b_{1c}}{\sqrt{n}} S_{12c}. \tag{14}$$

It should also be noticed that one pair of the parallel susceptances can be eliminated. In this case, $z_3 = 1$ and $b_{pic} = -2b_{1c}$.

3) DLE Network: The equations enabling the realization of a magic-T are

$$nz_1 \sin\theta_{1c} = -z_2 \sin\theta_{2c};$$

$$x_{12c} = \frac{(b_{p1c} + y_1 t_{1c}) + (b_{p2c} + y_2 t_{2c})}{1 + (b_{p1c} + y_1 t_{1c})(b_{p2c} + y_2 t_{2c})}, \tag{15a}$$

$$1 - (b_{p1c} + y_1 t_{1c})(b_{p1c} - y_1 t_{1c}^{-1}) = n[1 - (b_{p2c} + y_2 t_{2c})(b_{p2c} - y_2 t_{2c}^{-1})], \tag{15b}$$

$$|S_{14c}|^2 = \frac{x_{12c}^2}{x_{12c}^2 + nz_1^2 \sin^2\theta_{1c}}. \tag{15c}$$

As is seen, the conditions (15a)–(15c) create large freedom in the selection of the coupler elements. Particularly, the elimination of b_{p1} or b_{p2} simplifies the construction of the coupler.

C. Transdirectional Couplers ($S_{11} = S_{12} = 0$)

The LE, LDE, and DLE networks which fulfill the conditions required for a transdirectional signal transmission are analogous to the corresponding COD couplers. The only difference is that, for $n \neq 1$, the output ports are terminated with unequal impedances, which can sometimes be of practical interest. The equations which describe particular types of the coupler are as follows:

1) LE Network

$$b_{1c} = nb_{2c};\quad x_{12c} = \frac{1}{b_{1c} + b_{p1c}} = -\frac{1}{b_{2c} + b_{p2c}};$$

$$x_{12c}^2 = \frac{1}{nb_{2c}^2 - 1}, \tag{16a}$$

$$S_{13c}^2 = \frac{1}{\sqrt{n}b_{2c}x_{12c}} = \pm\frac{1}{\sqrt{1 + x_{12c}^2}}. \tag{16b}$$

2) LDE Network

$$z_3 \tan\theta_{3c} = \frac{1}{b_{1c} + b_{p1c}} = \frac{1}{b_{2c} + b_{p2c}};\quad b_{1c} = nb_{2c};$$

$$z_3^2 \sin^2\theta_{3c} = \frac{1}{nb_{2c}^2 - 1}, \tag{17a}$$

$$S_{13c} = \frac{1}{\sqrt{n}b_{2c}z_3 \sin\theta_{3c}} = \pm\frac{1}{\sqrt{1 + z_3^2 \sin^2\theta_{3c}}}. \tag{17b}$$

3) DLE Network

$$nz_1 \sin\theta_{1c} = z_2 \sin\theta_{2c};$$

$$(x_{12c})^{-1} = b_{p1c} - y_1 \cot\theta_{1c} = b_{p2c} - y_2 \cot\theta_{2c}, \tag{18a}$$

$$x_{12c}^2 = \frac{nz_1^2 \sin^2\theta_{1c}}{1 - nz_1^2 \sin^2\theta_{1c}}, \tag{18b}$$

$$S_{13c} = -\frac{\sqrt{n}z_1 \sin\theta_{1c}}{x_{12c}} = \mp\frac{1}{\sqrt{1 + x_{12c}^2}}. \tag{18c}$$

The above equations assure quadrature of the output signals. It should be remarked that, as in the case of the CD couplers, the realization of this type of coupler with magic-T properties is impossible.

The analysis presented above considers the couplers with the reactive components of the determined type (inductive or capacitive). More complex combinations of elements are also possible. An increased number of degrees of freedom in the design enables the shaping of the frequency characteristics. For instance, the replacement of the single reactive elements by series or parallel resonant circuits assures the specified power division between the output ports at two different frequencies.

IV. Example of Derivative Structure, Three-Branch Lumped-Element Coupler

Directional networks analyzed so far achieve good matching and isolation around the center frequency only and are to a large extent band-limited. This drawback can be overcome by applying cascade or tandem connections of the couplers. In such a way a three-branch coupler can be realized. The simplest way to derive the design equa-

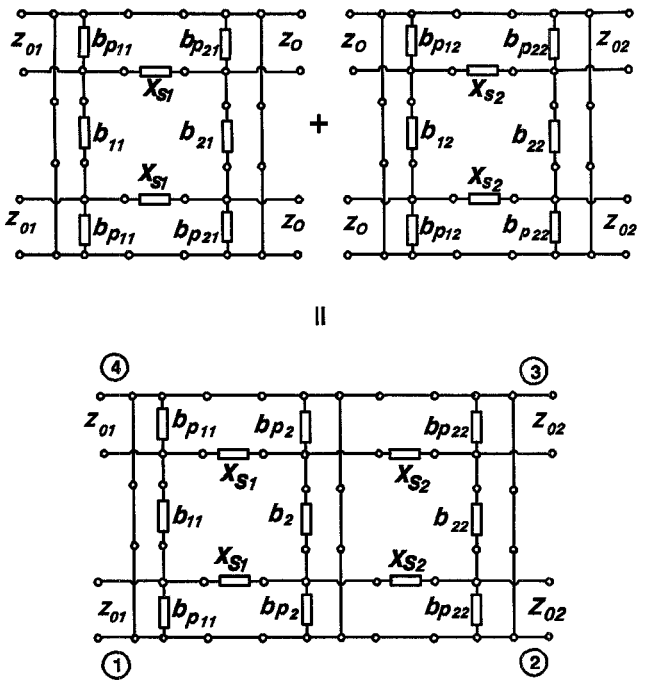

Fig. 5. Three-branch LE coupler as a cascade connection of two-branch couplers.

tions for a three-branch LE codirectional coupler is to consider a three-section network as a cascade connection of two separate two-branch couplers which, in general, have different coupling coefficients c_i and transformation ratios n_i (Fig. 5). The coupling coefficients (6) are defined as

$$c_i = \sqrt{n} b_{2ic} x_{sic} = \pm\sqrt{1 - x_{sic}^2} \qquad (i = 1, 2) \quad (19)$$

where $n_i = (Z_{oi}/Z_o)^{(-1)^i}$. The subscript c has the same meaning as before. The transformation ratio of the resultant three-branch coupler is equal $n = Z_{o2}/Z_{o1} = n_1 \cdot n_2$. To derive the coupling coefficient of the three-branch coupler, one has to determine a scattering matrix of the cascade connection of two contributing couplers. This matrix can be derived by using the technique described in [11]. For our purpose, the derivation at the center frequency is sufficient. The scattering coefficient representing the coupling, obtained as a result of the calculations, is equal to

$$S_{13} = \mp j(x_{s1c}\sqrt{1 - x_{s2c}^2} + x_{s2c}\sqrt{1 - x_{s1c}^2}). \quad (20)$$

In principle, any coupling value may be realized. An arbitrary choice of one series element (x_{s1c} or x_{s2c}) is also allowable; however, for simplicity, further considerations will be limited to the case of equal couplings. This leads to the assumption

$$x_{s1c} = x_{s2c} = x_{sc}.$$

Hence, (20) reduces to

$$S_{13} = C = \mp j2x_{sc}\sqrt{1 - x_{sc}^2}. \quad (21)$$

Then, for a 3-dB coupling, ($|S_{13c}| = 1/\sqrt{2}$), (7) yields two pairs of possible solutions for the series elements

$$x_{sc} = \pm\tfrac{1}{2}\sqrt{2 \pm \sqrt{2}}. \quad (22)$$

The above solutions, combined with (5) modified for the case of contributing couplers, lead to expressions describing the elements of the three-branch coupler. After impedance unnormalization, these expressions are

$$X_{sc1} = \pm\frac{\sqrt{n_1}Z_{o1}}{2}\sqrt{2 \pm \sqrt{2}} = \frac{1}{\sqrt{n}}x_{sc2}, \quad (23a)$$

$$B_{11c} = \pm\frac{1}{Z_{o1}}(\sqrt{2} \mp 1) = nB_{22c}, \quad (23b)$$

$$B_{2c} = B_{21c} + B_{12c} = \frac{2}{n_1}B_{11c}, \quad (23c)$$

$$B_{piic} = \frac{1}{X_{sic}} - B_{iic} \qquad (i = 1, 2), \quad (23d)$$

$$B_{p2} = \frac{1}{X_{sc1}} + \frac{1}{X_{sc2}} - B_{2c}. \quad (23e)$$

In particular, if the coupler has the form of Fig. 6, (23) can be rewritten as

$$L_{s1} = \frac{\sqrt{n_1}Z_{o1}}{4\pi f_c}\sqrt{2 \pm \sqrt{2}} = \frac{1}{\sqrt{n}}L_{s2}, \quad (24a)$$

$$L_{11} = \frac{Z_{o1}}{2\pi f_c}(\sqrt{2} \pm 1) = \frac{1}{n}L_{22} = \frac{2}{n_1}L_2, \quad (24b)$$

$$C_{pii} = \frac{1}{4\pi^2 f_c^2}\left(\frac{1}{L_{ii}} + \frac{1}{L_{si}}\right), \qquad (i = 1, 2), \quad (24c)$$

$$C_{p2} = \frac{1}{4\pi^2 f_c^2}\left(\frac{1}{L_2} + \frac{1}{L_{s1}} + \frac{1}{L_{s2}}\right). \quad (24d)$$

It is worthwhile pointing out that in the coupler design an additional degree of freedom exists, so the value of the internal impedance Z_o or some reactive element may be arbitrarily assumed. If, for instance, the value of C_{p11} (or C_{p22}) is chosen, one can calculate the transformation ratio n_1 from the following equation:

$$\sqrt{n_1} = \frac{\sqrt{2n}\sqrt{2 \pm \sqrt{2}}}{2\pi f_c C_{p22} Z_{o2}(\sqrt{2} \pm 1) - 1} \quad (25a)$$

or

$$\sqrt{n_1} = \frac{\sqrt{2}\sqrt{2 \pm \sqrt{2}}}{2\pi f_c C_{p11} Z_{o1}(\sqrt{2} \pm 1) - 1} \quad (25b)$$

Such a possibility is particularly attractive in the design of balanced amplifiers because the external capacitances of the coupler can be replaced by the input or output transistor capacitances.

In general, the internal transformation ratio (n_1) can be optimized to obtain the most convenient frequency characteristics of the coupler-transformer. The optimum value

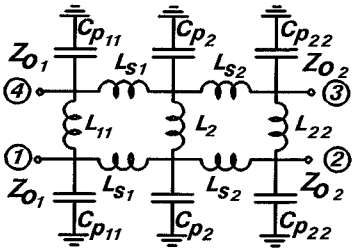

Fig. 6. Equivalent circuit of typical three-branch LE coupler-transformer.

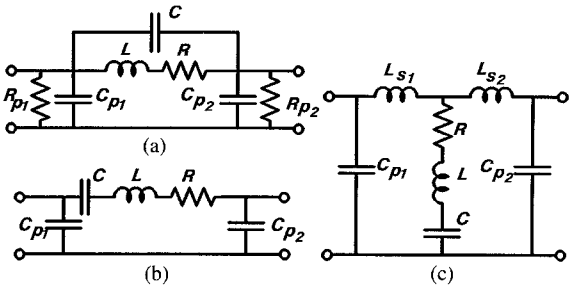

Fig. 7. Equivalent circuits of reactive lumped elements: (a) spiral or rectangular inductor, (b) series interdigital capacitor, (c) shunt interdigital capacitor.

is not necessarily the same as the value resulting from (25).

One may observe that the lower sign under the square root in (22)–(25) lead to impractical element values, as well as to very selective frequency responses.

It may also be noted that the three-branch LE coupler enables lower output impedances ($\sim 1\ \Omega$) than those achievable with the two-branch coupler-transformer.

V. Computer Simulation of Frequency Characteristics of the Couplers

In the analysis presented above it has been assumed that all contributing elements are ideal. In practice, the lumped elements cannot be represented as simple reactive one-port components, but all parasitic effects and losses have to be taken into account. The small inductances are realized as short pieces of high-impedance microstrip lines (up to 0.2 nH) or single-loop inductors (0.2–0.5 nH). The higher values (up to 10 nH) can be obtained by means of circular or rectangular spirals. The capacitances are realized as interdigitated (0.01–0.5 pF) or overlay (up to 100 pF) capacitors.

Fig. 7 shows equivalent circuits of typical reactive lumped elements employed in MICs and MMIC's. The available data concerning the design of lumped elements are rather limited to the selected, approximate, formulas. The commercial computer programs (e.g., Touchstone) allow calculations of the element response (e.g., *S*-matrix) versus frequency for fixed geometrical dimensions. To perform the design which could realize the theoretical, properties of the networks, the knowledge of the equivalent element representation (Fig. 7) is necessary. The best way to get such a description is to use the library developed by a foundry or by oneself. Another possibility is to fit the parameters of the equivalent circuit to the frequency response of the element using available simulators. In the calculations of the frequency characteristics presented below, an in-house library developed for spiral inductors has been used. The models of the lumped capacitors have been derived using the second method, mentioned above. The response of the interdigitated capacitors was calculated applying the corresponding algorithms given in [10] with the phase shift in the main line taken into account. The models of the overlay capacitors can be taken from Touchstone's element catalogue. However, it has been found that small value (< 1 pF) overlay

TABLE I
Element Values for Ideal Co-Directional Couplers at 10 GHz

Type	*Ls* [*nH*] or *Zs* [Ω]*	*Lc* [*nH*] or *Zc* [Ω]*	*Cp* [*pF*]
LE	0.56	0.8	0.77
LDE	35.4	0.8	0.32
DLE	0.56	50	0.45

*Characteristic impedance of $\lambda/4$ transmission line.

TABLE II
Element Values for Ideal Contradirectional Couplers at 10 GHz

Type	*Ls* [*nH*] or *Zs* [Ω]*	*Lc* [*nH*] or *Zc* [Ω]*	*Cc* [*pF*] or *Zc***	*Cp*1 [*pF*]	*Cp*2 [*pF*]	*Lp*2 [*nH*]
LE	1.13	1.13	0.23	0.45	—	—
LDE	70.7	1.13	0.23	0.23	—	1.13
DLE	1.13	70.7	70.7	0.23	0.23	—

*Characteristic impedance of $\lambda/4$ transmission line.
**Characteristic impedance of $\frac{1}{4}\lambda$ transmission line.

capacitors can also be represented as lossy capacitors with a determined *Q* factor. To illustrate the properties of different types of the directional couplers considered above, some computer simulations have been done. In the simulations GaAs substrate of the thickness 0.1 mm has been taken with corresponding electrical parameters $\epsilon_r = 12.9$ and $\tan\delta = 0.001$.

Tables I and II present the component values which satisfy the conditions required for the idealized COD and CTD 3 dB couplers at the center frequency of 10 GHz. The corresponding values for other frequencies can easily be obtained by scaling. The TRD couplers, excluding the case of $n \neq 1$, are fully analogous to the COD couplers and are not discussed here. As one can see from the tables, in the majority of cases the capacitances are not higher than 0.5 pF and could be realized as interdigitated capacitors. The circuit representation of these elements (Fig. 7) is much more complicated than the model of the overlay capacitor. In the simulations, for simplicity, the shunting capacitive elements (with one exception men-

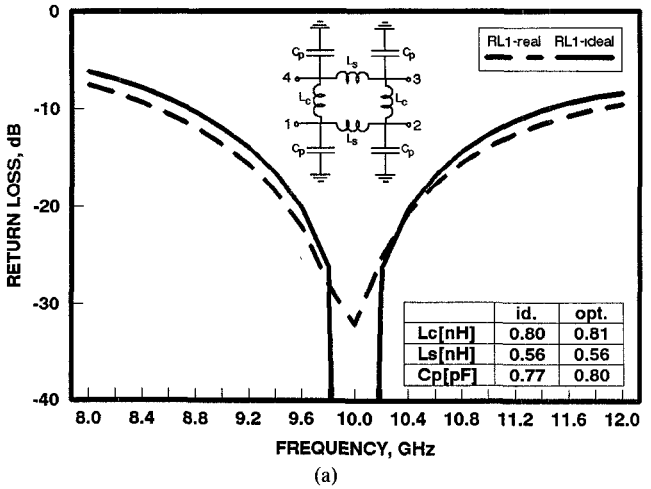

(a)

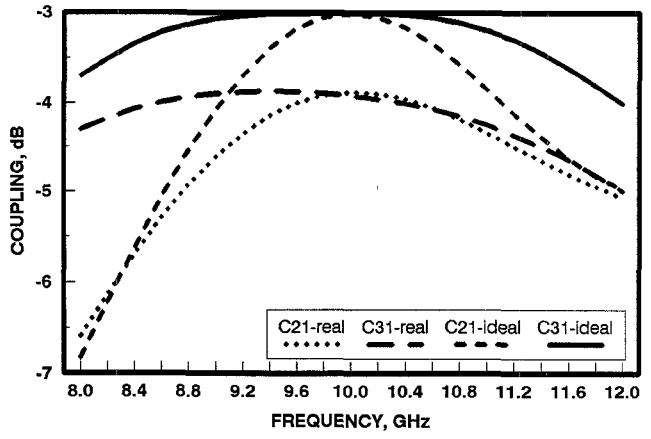

(b)

Fig. 8. Return loss (a) and couplings (b) of the LE COD 3 dB coupler.

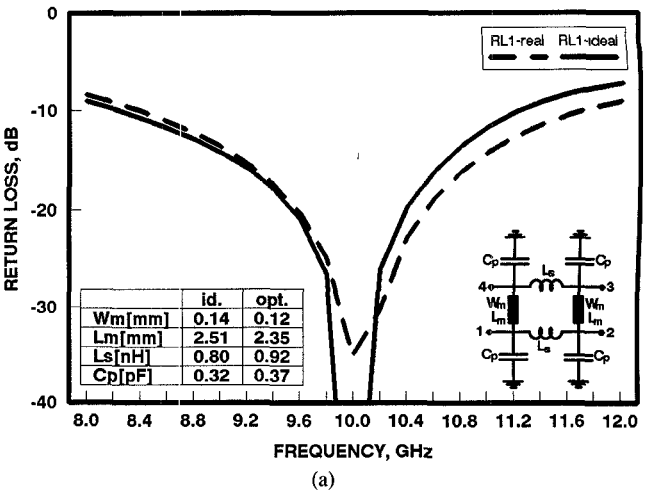

(a)

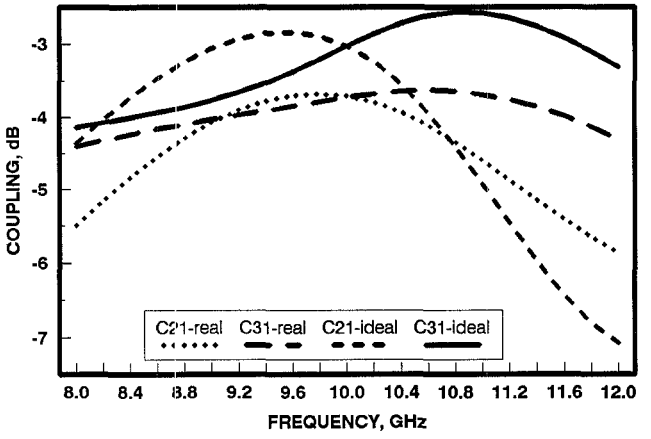

(b)

Fig. 9. Return loss (a) and couplings (b) of the DL COD 3 dB coupler.

tioned later) are represented as lumped capacitors with a finite Q value (e.g., $Q = 50$).

The simulations performed for COD couplers show that the LE construction assures the best balance of the output signals and flatness of the responses. The performance of this circuit is very similar to that of the classical two branch-line coupler. The characteristics of the LDE and DLE couplers are asymmetrical about the center frequency; this behavior is analogous to that of the two branch-line couplers with the line lengths different from $\lambda/4$ [5]. Figs. 8 and 9 show the frequency characteristics of the example COD (LE and DLE) couplers. The characteristics representing the ideal case (lossless elements, non-dispersive transmission lines, no discontinuities) are given as a reference. To make the frequency behavior of the real couplers similar to the ideal characteristics, the values of the elements have to be reoptimized. The changes are not too great and result mainly from the shift of the center frequency due to the parasitic reactive components. The figures show also the loss contributions which at the center frequency do not exceed 0.8 dB.

The frequency properties of the 3-dB couplers presented here are also representative of couplers with different coupling and transforming ratios.

Figs. 10 and 11 illustrate the frequency properties of the selected 3-dB CTD couplers. As before, the ideal characteristics are given as a reference. It has been found that the most attractive is the LDE coupler (Fig. 11). A particularly interesting feature of this coupler is a very good balance of the output signals over a relatively wide band. The imbalance is less than 0.5 dB in the octave band ($f/f_c = 0.75$–1.5). For the classical ($\frac{3}{2}\lambda$) ring coupler the same imbalance is achievable only over a 20% bandwidth. Owing to better properties and much less area occupied by the coupler, its use, particularly at lower frequencies, is more advantageous than a fully distributed line coupler. It has to be remarked that, in the simulation of the last coupler, all capacitors have been assumed as interdigitated and represented by the appropriate models. An example of the practical realization of such a coupler designed for S-band can also be found in [3].

Considering the three-branch coupler-transformers it can be seen (25) that the range of the transformation ratio is limited by the realizable values of inductances and capacitances at a given frequency. Assuming that an inductance of 3 nH is achievable at X-band and that the parasitic capacitances to ground can be included as an integral part of the coupler, the 50 Ω impedances can be trans-

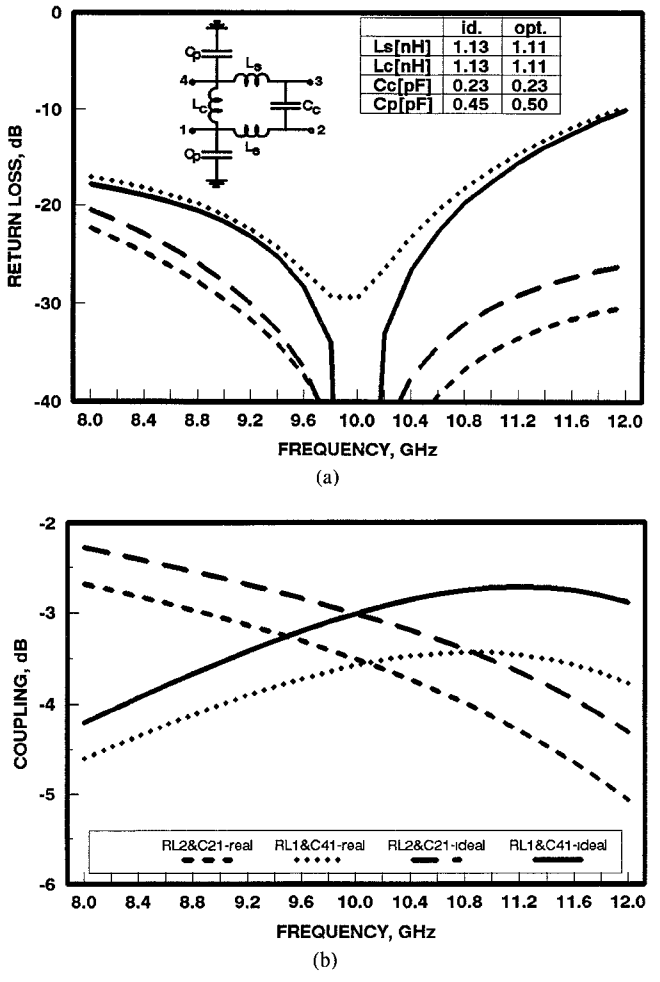

Fig. 10. Return losses (a) and couplings (b) of the LE CTR 3 dB coupler.

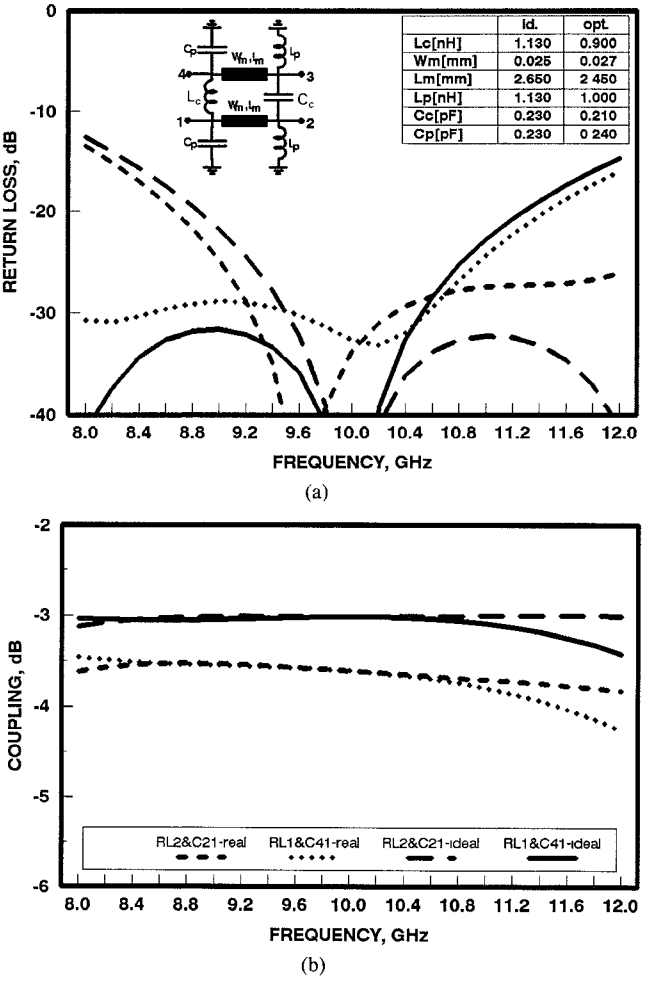

Fig. 11. Return losses (a) and couplings (b) of the LD CTD 3 dB coupler.

formed to the values as high as 150–200 Ω. The low impedance limit results from the capacitance values. Assuming a value of 10 pF as acceptable, the transformation of 50 Ω impedance to 1–2 Ω level at X-band seems to be realistic.

To illustrate the properties of the LE coupler-transformers, two- and three-branch 3-dB coupler-transformers have been designed for a center frequency of 10 GHz. Input and output impedances are respectively equal to 50 and 3 Ω ($n = 0.06$). The internal transformation ratio n_1 of the three-branch device was assumed equal to 0.13; this value assures symmetrical frequency characteristics. The element values of both couplers are: $L_1 = 0.8$ nH, $L_2 = 0.05$ nH, $L_{12} = 0.14$ nH, $C_{p1} = 2.2$ pF, $C_{p2} = 7.1$ pF for the three-branch coupler and $L_{11} = 1.92$ nH, $L_2 = 0.125$ nH, $L_{22} = 0.115$ nH, $L_{s1} = 0.265$ nH, $L_{s2} = 0.065$ nH, $C_{p11} = 1.09$ pF, $C_{p2} = 6.9$ pF, $C_{p22} = 6.1$ pF for the two-branch coupler. The VSWR's and couplings of both couplers are shown in Fig. 12. The bandwidth of the hybrids is mainly limited by the input VSWR and isolation between the output ports. For the two-branch coupler, and input VSWR of less than 2 to 1 with an isolation between output ports greater than 10 dB can be achieved only over an 5-percent bandwidth. For the three-branch

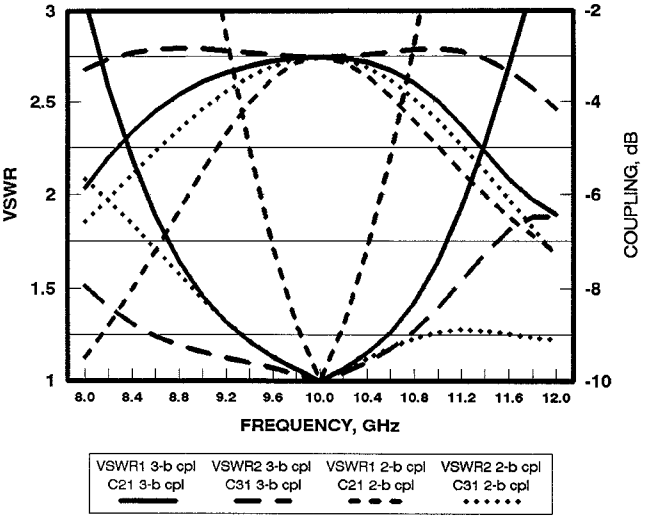

Fig. 12. VSWR's and couplings of LE 3 dB coupler-transformers.

coupler, the same parameters can be achieved over nearly a 30-percent bandwidth.

For comparison the frequency responses of the 3-dB LE three-branch coupler with equal terminating impedances and different values of $n_1 = 0.5$–0.75 have also been cal-

culated. The frequency dependence of the coupling is approximately similar to the characteristics shown in Fig. 12. The VSWR is lower than $VSWR_1$ but higher than $VSWR_2$ (Fig. 12) in the whole frequency band. The coupler performances can be optimized by varying the value of the internal transformation ratio n_1.

VI. Conclusion

The analysis presented in the paper shows that the conventional distributed four-port ring structures which include, among others, the branch line and rat-race couplers have lumped and lumped-distributed equivalents. All three types of directionality and quadrature and magic-T phase responses are achievable if the required conditions are fulfilled. The frequency properties of the lumped and lumped-distributed couplers are analogous to the distributed equivalents, particularly if compared to the couplers with the perimeters different from λ or $\frac{3}{2}\lambda$ [5].

The generality of the analysis enables the development of different types of couplers with interesting properties attractive for the applications in MIC an MMIC. The development of more complex directional structures based on the ring type sections is also possible. This is illustrated by the example of the LE three-branch coupler-transformer. The appropriate design equations are also given. It has been shown that a LE technique enables the transformation of a 50 Ω input impedance to the level of a few ohms at the coupler output ports. Such transformation ratios are not achievable using conventional branchline microstrip or stripline couplers. The added freedom in the design resulting from the three-branch structure enables the shaping of frequency characteristics or an arbitrary choice of some reactive elements. This last possibility can be useful in the design of balanced transistor amplifiers. The external coupler elements can be replaced by the transistor input and/or output reactances.

The equations presented in the paper concern the idealized reactive elements and are helpful in the preliminary design as well as in the choice of the most suitable form of the coupler-transformer. The final design should include realistic models of the elements and needs some refinement with the help of available simulators.

Appendix

Evaluation of the Directional Properties of Four-Port Networks

The four-port structures being used in microwave constructions are usually symmetrical about one plane at least. In the analysis, losslessness ($[S][S]_t^* = [U]$) and reciprocity ($[S] = [S]_t$) are assumed. The symmetry enables the even and odd mode analysis [7] to be applied. This method, expanded to multiport networks, allows one to determine the scattering matrix of the $2n$-port considering the set of the equivalent n-ports obtained as a result of the even and odd excitation of the selected pair of ports. The scattering coefficients are given by

$$S_{\substack{ij \\ i,2n+1-j}} = \tfrac{1}{2}(S_{ije} \pm S_{ijo}); \qquad i, j = 1, 2, \cdots n \tag{A1}$$

where subscripts "e" and "o" refer to the even and odd excitation, respectively. The signs "+" and "−" correspond to the upper and lower indices on the LHS, respectively. In the case of the four-port ($2n = 4$), assuming the port numeration according to Fig. 1, $S_{ije,o}$ coefficients of the equivalent two-port networks can be expressed by the corresponding coefficients of the wave-amplitude transmission matrix [8]

$$S_{11e,o} = \frac{T_{21e,o}}{T_{11e,o}}; \quad S_{12e,o} = \frac{1}{T_{11e,o}}; \quad S_{22e,o} = -\frac{T_{12e,o}}{T_{11e,o}}. \tag{A2}$$

The wave-amplitude transmission matrix is defined as [8]

$$\begin{bmatrix} a_1 \\ b_1 \end{bmatrix} = [T] \begin{bmatrix} b_2 \\ a_2 \end{bmatrix}. \tag{A3}$$

For reciprocal and lossless two-port networks, $T_{11} = T_{22}^*$ and $T_{12} = T_{21}^*$. The use of the transmission matrix simplifies the formulation of the conditions that a four-port be a directional coupler. Three types of directional couplers can be defined:

codirectional (COD) couplers, for which

$$S_{ii} = S_{14} = 0 \tag{A4}$$

contradirectional (CTD) couplers, for which

$$S_{ii} = S_{13} = 0, \tag{A5}$$

transdirectional (TRD) couplers, for which

$$S_{ii} = S_{12} = 0. \tag{A6}$$

It can be proved that for the COD coupler, the phases of the scattering coefficients are related according to

$$\angle S_{13} = \angle S_{12} + (2k + 1)\frac{\pi}{2}; \qquad k = 0, \pm 1, \pm 2 \cdots \tag{A7}$$

which means that the phase difference of the output signals is 90° and the four-port can be classified as a quadrature coupler. Combining (A4) and (A7) with (A1) and (A2) one obtains

$$T_{12e} = T_{12o} = 0. \tag{A8}$$

This condition, taking into account the unitary principle, results in

$$|T_{11e}|^2 = |T_{11o}|^2 = 1. \tag{A9}$$

Applying the same procedure to the CTD coupler one obtains

$$2\angle S_{12} = \angle S_{14} + \angle S_{23} + (2k + 1)\pi; \qquad k = 0, \pm 1, \pm 2 \cdots \tag{A10}$$

$$T_{11e} = T_{11o}; \quad T_{12e} = -T_{12o}. \tag{A11}$$

The additional condition

$$\Re T_{12e} = \Re T_{12o} = 0, \tag{A12}$$

leads to the following relations

$$S_{14} = S_{23}; \quad \angle S_{12} = \angle S_{14} + (2k + 1)\frac{\pi}{2} \tag{A13}$$

which indicate that the coupler is completely, electrically symmetrical and the phase difference of the output signals is 90°. However, the condition

$$\Im T_{12} = \Im T_{12o} = 0 \tag{A14}$$

makes the output signals of the coupler being in or out of phase, which is seen from the resulting expressions

$$S_{14} = -S_{23}; \quad \angle S_{12} = \arg S_{14} + k\pi. \tag{A15}$$

Such a four-port network is classified as a magic-T.

For the TRD coupler (A6), the unitary principle leads to expressions

$$2\angle S_{13} = \angle S_{14} + \angle S_{23} + (2k + 1)\pi, \quad k = 0, \pm 1, \pm 2 \cdots \tag{A16}$$

$$T_{11e} = -T_{11o}; \quad T_{12e} = T_{12o}. \tag{A17}$$

As previously, the conditions (A12) and (A14) make the coupler of the quadrature or magic-T type, respectively.

References

[1] M. Caulton *et al.*, "Status of lumped elements in microwave integrated circuits—present and future," *IEEE Trans. Microwave Theory Tech.*, vol. MTT-19, no. 7, pp. 538–599, July 1971.

[2] C. Y. Ho, "Lumped element quadrature coupler design," *Microwave J.*, vol. 22, no. 9, pp. 67–70, Sept. 1979.

[3] R. W. Vogel, "Directional couplers with lumped and distributed elements," in *Proc. 26 Intern. Wies. Koll., TH Ilmenau, Vortragsr. Mikrowellentechnik*, 1981, pp. 79–81.

[4] R. K. Gupta, W. J. Getsinger, "Quasi-lumped-element 3- and 4-port networks for MIC and MMIC applications," in *1984 IEEE MTT-S Int. Microwave Symp. Dig.*, San Francisco, pp. 409–411.

[5] R. W. Vogel, "Directional properties of four-port ring structure," *Archiwum Elektrotechniki*, t. XXVI, z. 1, pp. 107–120, 1977 (in Polish).

[6] R. Gupta *et al.*, "Impedance transforming 3-dB 90° hybrids," in *1987 IEEE MTT-5 Int. Microwave Symp. Dig.*, pp. 203–206.

[7] J. Reed, G. A. Wheeler, "A method of analysis of symmetrical four-port networks," *IEEE Trans. Microwave Theory Tech.*, vol. MTT-4, no. 4, pp. 246–252, Oct. 1956.

[8] R. E. Collin, Foundations for microwave engineering. New York: McGraw-Hill, 1966.

[9] E. Pettenpaul et al., "CAD models of lumped elements on GaAs up to 18 GHz," *IEEE Trans. Microwave Theory Tech.*, vol. 36, no. 2, pp. 294–304, Feb. 1988.

[10] F. Sellberg, "Simple and accurate algorithms to include Lange- and asymmetric microstrip couplers in CAD-packages," in *Proc. 18th Europ. Microwave Conf.*, Stockholm, 1988, pp. 1157–1162.

[11] T. A. Abele, "Über die streumatrix allgemeiner zusammengeschalteter mehrpole," *Arch. El. Übertrag*, Bd. 14, heft 6, pp. 161–168, 1960.

Ryszard W. Vogel (M'89–SM'91) was born in Lwow, Poland, in 1941. He received the M.Sc., Ph.D. (with honors) and the habilitation degrees from the Technical University of Gdansk, Poland, in 1965, 1971, and 1981, respectively.

From 1965 to 1981 he was an Instructor and then Assistant Professor at the Technical University of Gdansk working in the field of microwave theory and technique. From 1981 to 1990 he was a Senior Scientist in the Swedish Institute of Microelectronics (formerly the Institute of Microwave Technology). Currently he is with the NobelTech (formerly Bofors Electronics), Sweden. His research interests are in the areas of MIC's and MMIC's.